Contact Ratios and Transmission Errors of a Helical Gear Set with Involute-Teeth Pinion and Modified-Circular-Arc-Teeth Gear*

Yi-Cheng CHEN** and Chung-Biau TSAY**

Contact ratio (CR) and transmission error (TE) are two significant indices for gear tooth strength and dynamics. This work investigated the CR, contact teeth (CT) and TE of a helical gear pair, composed of an involute pinion and a modified circular-arc gear. Point contact and built-in parabolic TE are obtained due to the modification of the gear's tooth profile. Tooth contact analysis (TCA) is applied to determine the TE as well as the CR of the proposed helical gear set under various assembly condition. The effect of gear design parameters on the CRs and TEs are also investigated in numerical examples.

Key Words: Contact Ratio, Transmission Error, Helical Gear Set, Mathematical Model, Tooth Contact Analysis

1. Introduction

Contact ratio (CR) is an important gear design index for gear bending, load sharing and contact stress. A higher CR can reduce the stress and transmission error (TE) of the gear set, by distributing the load among neighboring teeth. Factors such as tooth addendum, pressure angle, tooth size and center distance variation can influence the CR. Increasing the tooth height increases the CR, whereas increasing the pressure angle usually decreases the CR. Therefore, applying the enlarged gear addendum usually attains a high CR gear set (CR more than 2.0). Several researchers[1]-[3] have studied the characteristics of high CR spur gears. On the other hand, the TE can be calculated by performing tooth contact analysis (TCA)[4]-[8]. While evaluating the actual CR, Falah et al.[9] compared the corresponding AGMA CR to the values calculated by a loaded tooth contact analysis for spiral bevel gear sets. In addition, Umeyama et al.[10] clarified the relationships between the loaded TEs and the two indices, actual CR and effective CR, of a helical gear pair.

A gear set with a higher CR may reduce its tooth loads, contact stress and root stress. A high CR gear set is generally not as sensitive to tooth profile errors as a low CR one. Besides, the TE and vibration of the gear set are reduced by the multiple teeth contact as the CR is increased. This feature allows us to design a gear set with a lower noise level. Liou et al.[11] reported that high CR spur gears minimize dynamic load better than low CR gears. Lin et al.[12] reported that the parabolic profile modification is preferable to linear profile modification for high CR gears. More recently, Kahraman and Blankenship[13] explored how involute profile CR affects the torsional vibration behavior of the spur gear pairs by measuring dynamic transmission error (DTE).

As well known, decreasing the gear pressure angle is also an effective method to obtain high-CR gear sets. In addition, increasing the sliding velocity and CR may incur a higher power loss; whereas, decreasing the pressure angle increases the bending and compressive stresses since the tooth thickness is reduced[1]. Photoelastic stress experiments[14] and finite element analysis[15] are normally conducted to estimate the stress distribution on gears. Moreover, the instantaneous contact teeth (ICT), which can also be determined by applying the TCA method, is an important design factor for impact mechanisms. In general, the ICT for spur gears, helical gears, spiral bevel gears and hypoid gears are typically one or two teeth. Our recent work[16] investigated the ICT and the average contact ratio (ACR) of the ZK-type dual-

* Received 9th March, 2000

** Department of Mechanical Engineering, National Chiao Tung University, Hsinchu 30010, Taiwan, R.O.C. E-mail: cbtsay@cc.nctu.edu.tw

lead worm and worm gear drive by applying the TCA method. According to our results, ZK-type dual-lead worm gear set possesses a high CR (between 3 and 4) which might be affected by variations of center distance and pressure angle.

The helical gear pair discussed herein consists of an involute pinion and a modified circular-arc gear. Our previous studies[17],[18] have investigated the basic characteristics of this type of helical gear set, including mathematical models, undercut conditions as well as built-in parabolic TEs and localized bearing contacts. In this follow-up study, the CR and contact teeth (CT) of the proposed helical gear set are determined based on the TCA results. In addition, several illustrative examples demonstrate the effectiveness of gear design parameters and assembly conditions that are relevant to CRs and TEs. Moreover, different types of built-in TE curves are obtained by varying the radius center of the circular-arc rack cutter that generates the gear.

2. Mathematical Model of the Proposed Helical Gear Set

2.1 Involute pinion tooth surface

In this study, the tooth surface of the pinion is an involute screw surface generated by a straight-edged rack cutter Σ_P, as shown in Fig. 1. Tsay[8] developed the position vector and unit normal vector of the involute helical pinion, $\boldsymbol{R}_1=(x_1, y_1, z_1)$ and $\boldsymbol{n}_1=(n_{x1}, n_{y1}, n_{z1})$, represented in coordinate system $S_1(X_1, Y_1, Z_1)$ as follows:

$$
\begin{aligned}
x_1&=(l_P\cos\alpha_n^{(P)}-a_P+r_1)\cos\phi_1\\
&\quad+(l_P\cos\alpha_n^{(P)}-a_P)\cos\alpha_n^{(P)}\sin\lambda_P\sin\phi_1,\\
y_1&=(l_P\cos\alpha_n^{(P)}-a_P+r_1)\sin\phi_1\\
&\quad-(l_P\cos\alpha_n^{(P)}-a_P)\cos\alpha_n^{(P)}\sin\lambda_P\cos\phi_1,\\
z_1&=(a_P\tan\alpha_n^{(P)}-l_P\sin\alpha_n^{(P)})\cos\lambda_P\\
&\quad+\left(\frac{a_P}{\cos\alpha_n^{(P)}\sin\alpha_n^{(P)}}-\frac{l_P}{\sin\alpha_n^{(P)}}\right)\tan\lambda_P\sin\lambda_P\\
&\quad+\frac{S_P}{2\cos\lambda_P}+r_1\phi_1\tan\lambda_P, \qquad (1)
\end{aligned}
$$

$$
\begin{aligned}
n_{x1}&=\sin\alpha_n^{(P)}\cos\phi_1+\cos\alpha_n^{(P)}\sin\lambda_P\sin\phi_1,\\
n_{y1}&=\sin\alpha_n^{(P)}\sin\phi_1-\cos\alpha_n^{(P)}\sin\lambda_P\cos\phi_1, \qquad (2)
\end{aligned}
$$

and

$$n_{z1}=\cos\alpha_n^{(P)}\cos\lambda_P.$$

Symbols l_P and u_P stand for the surface parameters of rack cutter Σ_P; a_P represents the rack cutter's dedendum proportion; S_P denotes the tooth space of Σ_P; $\alpha_n^{(P)}$ and λ_P represent the normal pressure angle and the lead angle of the pinion, respectively.

2.2 Modified gear tooth surface

On the other hand, the gear is a modified helical gear generated by an imaginary rack cutter, which has a circular-arc curve in its normal section and moves along a curved-template guide in the lengthwise direction of the gear during the manufacturing process, as depicted in Fig. 2. This novel type of helical gear is designated as "modified circular-arc helical gear" though its profile is actually a special curve due to the generating process. Based on our previous work[18], the crowning of tooth profile keeps the gear contact point in the middle region of the tooth surface even under assembly errors. In addition, hob cutters with a circular-arc curve instead of a straight edge in their normal sections will result in a pre-designed parabolic TE when the helical gear pair is meshing under an ideal assembly condition. Moreover, the TE of the helical gear pair is continuous without any jump even when axial-misalignments occur.

2.2.1 Rack cutter surface Σ_G for modified circular-arc helical gear

The circular-arc normal section of the rack cutter Σ_G, used for manufacturing the modified circular-arc helical gear, is shown in Fig. 2(a). In Fig. 2(a), parameters A and C determine the initial and end points of the circular-arc curve, respectively, and S_G is the tooth thickness measured along the pitch circle. Symbol θ_G is a design parameter of the rack cutter, ranging from $\theta_{\min}^{(G)}$ to $\theta_{\max}^{(G)}$, $\alpha_n^{(G)}$ represents the normal

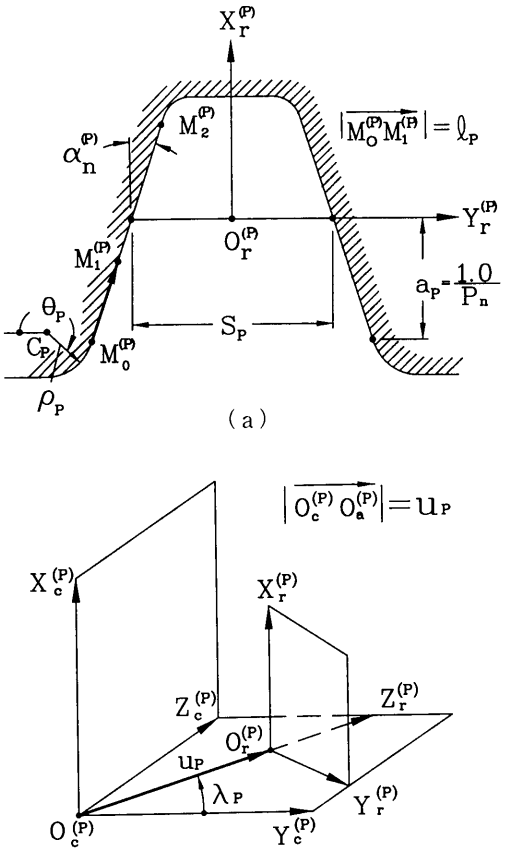

Fig. 1 Formation of rack cutter surface Σ_P

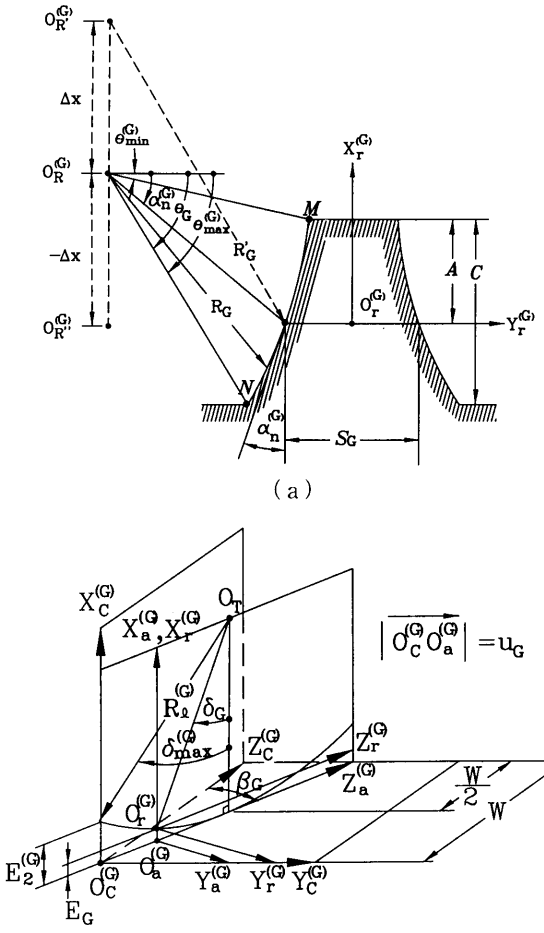

(a)

(b)

Fig. 2 Formation of rack cutter surface Σ_G

pressure angle, and R_G denotes the radius of the circular arc.

Practically, a curved-template guide may be imposed on a conventional hobbing machine to control the movement of the hob cutter. The shift of the hob cutter causes a crowning effect on the tooth flank. Figure 2(b) illustrates the formation of the three-dimensional rack cutter surface Σ_G. An auxiliary coordinate system $S_a^{(G)}(X_a^{(G)}, Y_a^{(G)}, Z_a^{(G)})$ which translates along line $\overline{O_c^{(G)}O_a^{(G)}}$ (i.e. axis $Z_a^{(G)}$) is set up. The normal section of the circular-arc rack cutter is rigidly attached to coordinate system $S_r^{(G)}$ with its origin $O_r^{(G)}$ moving along a curve of radius $R_l^{(G)}$ which has the same shape as the curved-template guide. Besides, coordinate system $S_c^{(G)}(X_c^{(G)}, Y_c^{(G)}, Z_c^{(G)})$ is rigidly attached to the transverse section of the rack cutter, and coordinate system $S_r^{(G)}(X_r^{(G)}, Y_r^{(G)}, Z_r^{(G)})$ is attached to coordinate system $S_c^{(G)}$ with a variable shifted amount E_G. The angle β_G, formed by axes $Z_a^{(G)}$ and $Z_c^{(G)}$ in plane $Z_c^{(G)}$-$Y_c^{(G)}$, is the helix angle of the generated helical gear. Parameter δ_G indicates the position on the curved-template guide and E_G is the corresponding shifted amount of the hob. Parameter

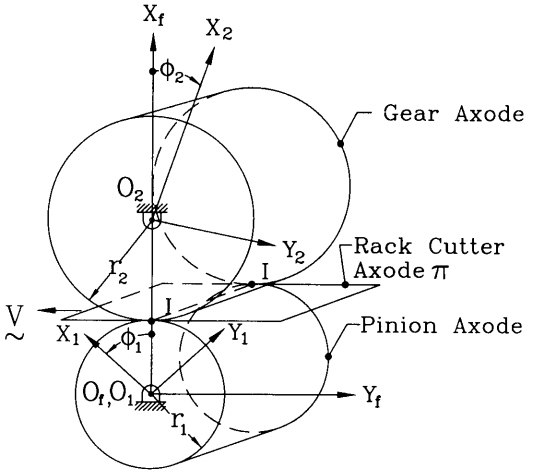

Fig. 3 Axodes relationship among the rack cutter, pinion and gear

$\delta_{\max}^{(G)}$ denotes the extreme value of δ_G at which parameter E_G reaches its maximum value $E_2^{(G)}$. Parameter W represents the face width of the gear.

Therefore, the imaginary rack cutter surface Σ_G and its unit normal vector can be represented in coordinate system $S_c^{(G)}$ as follows[17]:

$$\begin{aligned} x_c^{(G)} &= R_G(\sin\alpha_n^{(G)} - \sin\theta_G) + R_l^{(G)}(1-\cos\delta_G), \\ y_c^{(G)} &= -\left[R_G(\cos\alpha_n^{(G)} - \cos\theta_G) + \frac{S_G}{2}\right]\cos\beta_G \\ &\quad + R_l^{(G)}(\sin\delta_{\max}^{(G)} - \sin\delta_G)\sin\beta_G, \qquad (3) \\ z_c^{(G)} &= \left[R_G(\cos\alpha_n^{(G)} - \cos\theta_G) + \frac{S_G}{2}\right]\sin\beta_G \\ &\quad + R_l^{(G)}(\sin\delta_{\max}^{(G)} - \sin\delta_G)\cos\beta_G. \end{aligned}$$

$$\begin{aligned} n_{xc}^{(G)} &= A_G(\cos\delta_G\sin\theta_G), \\ n_{yc}^{(G)} &= A_G(\sin\delta_G\sin\theta_G\sin\beta_G \\ &\quad - \cos\delta_G\cos\theta_G\cos\beta_G), \qquad (4) \end{aligned}$$

and

$$\begin{aligned} n_{zc}^{(G)} &= A_G(\sin\delta_G\sin\theta_G\cos\beta_G \\ &\quad + \cos\delta_G\cos\theta_G\sin\beta_G), \end{aligned}$$

where

$$A_G = (\sin^2\theta_G + \cos^2\delta_G\cos^2\theta_G)^{-\frac{1}{2}}.$$

2.2.2 Modified circular-arc helical gear tooth surface

The locus of instantaneous axes of rotation represented in a coordinate system attached to a movable body is known as the body axode. Figure 3 illustrates the relationships among the rack cutter axodes and the corresponding generated pinion and gear axodes. In Fig. 3, cylinders of pitch radii r_1 and r_2 are the pinion and gear axodes, and plane π, tangent to both cylinders, is the axode of the rack cutter. The line of tangency of the axodes, I - I, represents the instantaneous axis of gear rotation. In the generating process, the rack cutter translates with velocity V while the pinion and the gear rotate with angles ϕ_1 and ϕ_2, respectively.

Based on the theory of gearing, the generated gear surface can be obtained by simultaneously considering the equation of meshing and the locus of the imaginary rack cutter represented in coordinate system S_2. Thus, the mathematical model of the generated gear tooth surface can be expressed by Ref.(17):

$$x_2=(x_c^{(G)}-r_2)\cos\phi_2+(y_c^{(G)}-r_2\phi_2)\sin\phi_2,$$
$$y_2=-(x_c^{(G)}-r_2)\sin\phi_2+(y_c^{(G)}-r_2\phi_2)\cos\phi_2, \quad (5)$$
$$z_2=z_c^{(G)},$$

and

$$f_2(\phi_2,\theta_G,\delta_G)=\left\{r_2\phi_2+\left[R_G(\cos\alpha_n^{(G)}-\cos\theta_G)+\frac{S_G}{2}\right]\cos\beta_G-R_l^{(G)}(\sin\delta_{\max}^{(G)}-\sin\delta_G)\sin\beta_G\right\}\times\cos\delta_G\sin\theta_G+[R_G(\sin\alpha_n^{(G)}-\sin\theta_G)+R_l^{(G)}(1-\cos\delta_G)](\sin\delta_G\sin\theta_G\sin\beta_G-\cos\delta_G\cos\theta_G\cos\beta_G)=0, \quad (6)$$

where $x_c^{(G)}$, $y_c^{(G)}$ and $z_c^{(G)}$ are expressed in Eq.(3); ϕ_2 is the gear's rotational angle during the generating process; and r_2 denotes the pitch radius of the generated gear.

The unit normal vector of the modified circular-arc helical gear tooth surface, represented in coordinate system S_2, can be expressed by

$$n_{x2}=n_{xc}^{(G)}\cos\phi_2+n_{yc}^{(G)}\sin\phi_2,$$
$$n_{y2}=-n_{xc}^{(G)}\sin\phi_2+n_{yc}^{(G)}\cos\phi_2, \quad (7)$$

and $n_{z2}=n_{zc}^{(G)}$.

2.2.3 Simulation of gear meshing

To simulate the meshing of a helical gear pair, the position and unit normal vectors of the pinion and gear tooth surfaces must be represented in the same coordinate system, say, coordinate system $S_f(X_f, Y_f, Z_f)$. Besides, assembly errors including center distance error and axial misalignments may occur in practical applications of helical gear sets. Figure 4 shows the relationships among the coordinate systems $S_f(X_f, Y_f, Z_f)$, $S_1(X_1, Y_1, Z_1)$, $S_2(X_2, Y_2, Z_2)$, $S_h(X_h, Y_h, Z_h)$ and $S_v(X_v, Y_v, Z_v)$ when center distance error and axial misalignments occur. Coordinate systems S_1 and S_2 are rigidly connected to the pinion and gear, respectively; S_h and S_v are the reference coordinate systems to simulate the horizontal and vertical axial misalignments, respectively; and S_f is the fixed coordinate system. In Fig. 4, angles ϕ_1' and ϕ_2' are the rotational angles of the pinion and gear when meshed with assembly errors. Figure 4 also considers assembly errors of horizontal misaligned angle $\Delta\gamma_h$ with respect to the coordinate system S_f, vertical misaligned angle $\Delta\gamma_v$ with respect to the coordinate system S_h and center distance error ΔC.

By applying the homogeneous coordinate transformation equations and vector transformation equations, the position vector and unit normal vector of the involute helical pinion represented in the fixed coordinate system $S_f(X_f, Y_f, Z_f)$ are obtained as follows:

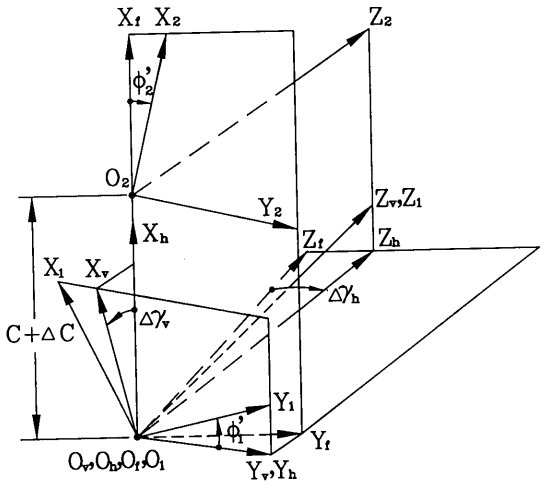

Fig. 4 Coordinate systems for gear pair simulation with assembly errors

$$x_f^{(1)}=b_1\cos\Delta\gamma_v+z_1\sin\Delta\gamma_v,$$
$$y_f^{(1)}=-a_1\cos\Delta\gamma_h-(b_1\sin\Delta\gamma_v-z_1\cos\Delta\gamma_v)\sin\Delta\gamma_h,$$
$$z_f^{(1)}=a_1\sin\Delta\gamma_h-(b_1\sin\Delta\gamma_v-z_1\cos\Delta\gamma_v)\cos\Delta\gamma_h, \quad (8)$$

and

$$n_{fx}^{(1)}=d_1\cos\Delta\gamma_v+n_{z1}\Delta\sin\gamma_v,$$
$$n_{fy}^{(1)}=-c_1\cos\Delta\gamma_h-(d_1\sin\Delta\gamma_v-n_{z1}\cos\Delta\gamma_v)\sin\Delta\gamma_h,$$
$$n_{fz}^{(1)}=c_1\sin\Delta\gamma_h-(d_1\sin\Delta\gamma_v-n_{z1}\cos\Delta\gamma_v)\cos\Delta\gamma_h, \quad (9)$$

where

$$a_1=x_1\sin\phi_1'-y_1\cos\phi_1',$$
$$b_1=x_1\cos\phi_1'+y_1\sin\phi_1',$$
$$c_1=n_{x1}\sin\phi_1'-n_{y1}\cos\phi_1',$$
$$d_1=n_{x1}\cos\phi_1'+n_{y1}\sin\phi_1'.$$

Similarly, the position vector and unit normal vector of the modified circular-arc helical gear represented in the fixed coordinate system $S_f(X_f, Y_f, Z_f)$ are expressed as follows:

$$x_f^{(2)}=x_2\cos\phi_2'-y_2\sin\phi_2'+C',$$
$$y_f^{(2)}=x_2\sin\phi_2'-y_2\cos\phi_2', \quad (10)$$
$$z_f^{(2)}=z_2,$$

and

$$n_{fx}^{(2)}=n_{x2}\cos\phi_2'-n_{y2}\sin\phi_2',$$
$$n_{fy}^{(2)}=n_{x2}\sin\phi_2'+n_{y2}\cos\phi_2', \quad (11)$$
$$n_{fz}^{(2)}=n_{z2},$$

where $C'=C+\Delta C$ represents the center distance of the helical gear set when center distance error ΔC exists.

3. Transmission Errors and Contact Ratios

When the helical pinion and gear are meshing with each other, the mating surfaces must satisfy the

condition of continuous tangency at the contact point[5),6)]. Continuous tangency can be ensured if the position vectors and unit normal vectors of the two mating surfaces coincide with each other at any meshing instant. Thus,

$$\boldsymbol{R}_f^{(1)}=\boldsymbol{R}_f^{(2)}, \tag{12}$$

and

$$\boldsymbol{n}_f^{(1)}=\boldsymbol{n}_f^{(2)}, \tag{13}$$

where $\boldsymbol{R}_f^{(1)}$ and $\boldsymbol{R}_f^{(2)}$ denote the position vectors of the pinion and gear tooth surfaces represented in coordinate system S_f, respectively; and $\boldsymbol{n}_f^{(1)}$ and $\boldsymbol{n}_f^{(2)}$ are the unit normal vectors of the pinion and gear tooth surfaces, respectively, represented in coordinate system S_f.

In a three-dimensional space, Eqs.(12) and (13) form a system of five independent nonlinear equations with six unknowns since $|n_f^{(1)}|=|n_f^{(2)}|=1$. This system of nonlinear equations can be solved by selecting one of the unknowns as an input variable. Generally, the pinion's rotational angle, ϕ_1', is chosen as the input variable when solving the system of nonlinear equations with Newton-Raphson algorithm. Consequently, the rotational angle of an output gear, ϕ_2', is a function of ϕ_1' and thus can be written as $\phi_2'(\phi_1')$. For the ideal meshing condition, $\phi_2'=\phi_1'N_1/N_2$, i.e., the gear rotational angle is the product of the pinion's rotational angle and the pinion-gear ratio. Function $\phi_2'(\phi_1')$ is a nonlinear function and its deviation from $\phi_1'N_1/N_2$ is defined as the TE of the gear pair:

$$\Delta\phi_2'(\phi_1')=\phi_2'(\phi_1')-\phi_1'\frac{N_1}{N_2}, \tag{14}$$

where N_1 and N_2 denote the teeth numbers of the pinion and gear, respectively, and $\Delta\phi_2'(\phi_1')$ represents the TE of the gear drive induced by assembly or manufacturing errors.

Conventionally, the CR of a gear pair is described as the average number of teeth in contact during the gear meshing. CR is also defined as the length of contact path along the line of action to be divided by the base pitch[19)]. In general, a gear set with a minimum CR of 1.4 is desirable, and it should never be less than 1.2. As well known, the meshing of a spur gear set has only a transverse CR; whereas the CR of a conventional helical gear set is the sum of transverse CR and face CR. However, based on our previous study[18)], point contact replaces line contact for the proposed helical gear set. Localization of the bearing contact is accompanied with a reduction of CR since the number of potential contact ellipses is reduced. Basically, the CR can be defined by the gear's rotational angle, measured from the starting point of contact to the end point of contact, to be divided by the angle formed by the adjacent two teeth. Therefore, the CR for the proposed helical gear set can be calculated from the TCA results and expressed by the following equation[6)]:

$$m_c=\frac{\Delta\phi_1'N_1}{360^\circ}, \tag{15}$$

where $\Delta\phi_1'$ is the pinion's rotational angle while one pair of teeth is in mesh within the range of tooth surfaces. Angle $\Delta\phi_1'$ can be determined based on the TCA simulation results. TCA computer program is adapted to evaluate the CRs as well as TEs of the proposed helical gear set when the contact teeth are in mesh within the tooth surfaces.

4. Illustrative Examples

Some examples are given below to calculate the TEs and CRs of the proposed helical gear set under various meshing conditions. Table 1 lists the major design parameters of the helical gear set used in these cases. To simulate the assembly errors, three parameters, ΔC, $\Delta\gamma_v$, and $\Delta\gamma_h$ are considered in the meshing process, where ΔC denotes the center distance deviation, $\Delta\gamma_v$ and $\Delta\gamma_h$ represent the vertical and horizontal misaligned angles, respectively. The TCA, TEs and CRs are calculated based on the one-tooth contact judgment and rigid body motion is considered for the pinion and gear tooth surfaces.

4.1 Gear set meshing under various assembly conditions

When two TE curves are coupled, the instantaneous contact teeth (ICT) is two; otherwise, ICT is one. Usually, the ICT of spur and helical gear sets is between one or two teeth and is also defined on the basis of the TE curves of the gear set. Figure 5 illustrates the contact teeth (CT) and TE of the gear set under ideal assembly condition (i.e., no assembly error). According to this figure, the contact of the gear pair begins at $\phi_1'=-12.5^\circ$ and ends at $\phi_1'=18.3^\circ$. Consequently, the CR of the proposed gear set, calculated by Eq.(15), is 1.54 under ideal meshing condition. Figure 5 also reveals that the CT varies between one tooth and two teeth during the meshing process. This same figure indicates that the proposed modified helical gear set exhibits a designed parabolic TE

Table 1 Major design parameters of the proposed modified helical gear pair

Parameters \ Design Values	Pinion	Gear
Number of Teeth	18	36
Helix Angle	15°(LH)	15°(RH)
Pressure Angle, Normal	20°	20°
Module, Normal	4.0 mm	4.0 mm
Radius of Curved-Template Guide $R_f^{(G)}$	straight-Edged	200mm
Radius of Rack Cutter Normal Section R_G	straight-Edged	1000mm
Face Width	40mm	40mm

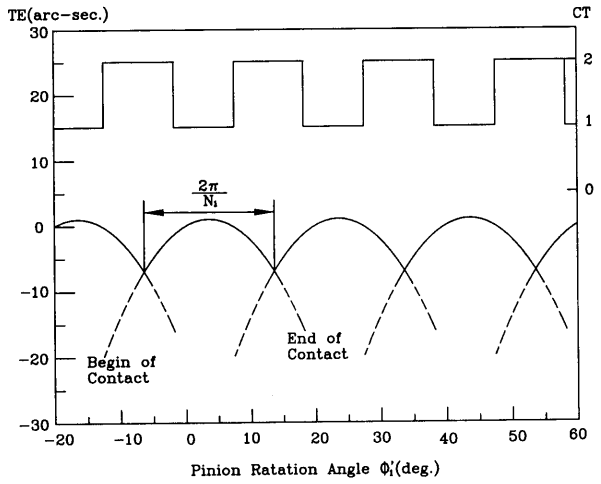

Fig. 5 Contact teeth and transmission error of the gear pair under ideal assembly condition

under ideal meshing condition.

Table 2 summarizes the CRs and magnitudes of TEs of the proposed helical gear set under several assembly conditions. For an ideal meshing condition, the CR is 1.54 and the TE for one meshing cycle is 8.119 arc-sec. When a positive horizontal axial misalignment $\Delta\gamma_h=0.1°$ occurs, the beginning and end angles of contact become $-13.0°$ and 17.7°, respectively, and the TE is 8.116 arc-sec. In addition, the beginning and end angles of contact become $-11.9°$ and 18.8°, respectively, and the TE becomes 8.143 arc-sec, when a negative horizontal misaligned angle $\Delta\gamma_h=-0.1°$ is present. However, according to Table 2, the CRs for the gear set under these two horizontal axial misalignments are the same and equal 1.535 in both cases.

As Table 2 illustrates, when a positive vertical misaligned angle $\Delta\gamma_v=0.15°$ is present, the CR increases from 1.54 to 1.55. By contrast, the CR decreases from 1.54 to 1.525 when a negative vertical misaligned angle $\Delta\gamma_v=-0.15°$ is present. Furthermore, a negative center distance error $\Delta C=-0.3$ mm increases the CR from 1.54 to 1.61. On the other hand, for a gear set with a positive center distance variation $\Delta C=0.3$ mm, the CR decreases from 1.54 to 1.47. Our results also indicate that the magnitude of TE decreases when a positive center distance is present. In sum, although a horizontal axial misalignment $\Delta\gamma_h$ reduces the CR of the gear set, both negative center distance variation and positive vertical axial misalignment increase the CR. Moreover, the assembly errors only affect the magnitude of TE slightly.

4.2 Effects of design parameters on contact ratios

Tables 3, 4 and 5 demonstrate how the design parameters, including pressure angle(PA), radius of circular-arc rack cutter R_G, radius of curved-template guide $R_l^{(G)}$ and helix angle(HA), affect the CRs of the proposed gear set. The above mentioned design parameters are depicted in Fig. 2. Our results show that the CRs decrease with an increase of helix angles. In addition, a gear set with a larger pressure angle results in a smaller CR. Besides, the CRs with $R_G=$ 1 000 mm are slightly smaller than those of $R_G=350$

Table 2 Contact ratios and transmission errors of the gear set under several assembly conditions

Assembly Conditions			Begin Contact Angle (Deg.)	End Contact Angle (Deg.)	Contact Ratio	Transmission Error (Arc-Sec.)
ΔC (mm)	$\Delta\gamma_h$ (Deg.)	$\Delta\gamma_v$ (Deg.)				
0	0	0	-12.5	18.3	1.540	8.119
0	0.10	0	-13.0	17.7	1.535	8.116
0	-0.10	0	-11.9	18.8	1.535	8.143
0	0	0.15	-12.4	18.6	1.550	8.088
0	0	-0.15	-12.6	17.9	1.525	8.110
0.3*	0	0	-11.5	17.9	1.470	7.986
-0.3*	0	0	-13.5	18.7	1.610	8.119

* $\Delta C=0.3mm$ is 0.268 % of center distance variation

Table 3 Contact ratios under several gear parameters for the case $R_l^{(G)}=100$ mm

PA / R_G / CR / HA	20°		22.5°		25°	
	R_G=350 (mm)	R_G=1000 (mm)	R_G=350 (mm)	R_G=1000 (mm)	R_G=350 (mm)	R_G=1000 (mm)
0°	1.625	1.615	1.540	1.520	1.470	1.450
5°	1.615	1.605	1.530	1.515	1.460	1.440
10°	1.595	1.575	1.510	1.490	1.440	1.415
15°	1.555	1.530	1.470	1.445	1.400	1.375
20°	1.495	1.475	1.415	1.385	1.345	1.315

Table 4 Contact ratios under several gear parameters for the case $R_l^{(G)}=200$ mm

PA / R_G / CR / HA	20°		22.5°		25°	
	R_G=350 (mm)	R_G=1000 (mm)	R_G=350 (mm)	R_G=1000 (mm)	R_G=350 (mm)	R_G=1000 (mm)
0°	1.625	1.615	1.540	1.520	1.470	1.450
5°	1.615	1.605	1.530	1.515	1.460	1.440
10°	1.595	1.575	1.510	1.490	1.440	1.420
15°	1.565	1.540	1.480	1.450	1.410	1.375
20°	1.515	1.475	1.435	1.390	1.365	1.320

Table 5 Contact ratios under several gear parameters for the case $R_l^{(G)}=500$ mm

PA / R_G / CR / HA	20°		22.5°		25°	
	R_G=350 (mm)	R_G=1000 (mm)	R_G=350 (mm)	R_G=1000 (mm)	R_G=350 (mm)	R_G=1000 (mm)
0°	1.625	1.615	1.540	1.520	1.470	1.450
5°	1.625	1.605	1.540	1.520	1.465	1.445
10°	1.615	1.585	1.530	1.500	1.460	1.420
15°	1.595	1.550	1.510	1.460	1.450	1.390
20°	1.545	1.510	1.495	1.415	1.430	1.345

Table 6 Effects of pressure angle on contact ratios and transmission errors

Pressure Angle (Deg.)	Begin Contact (Deg.)	End Contact (Deg.)	Contact Ratio	Transmission Error (Arc-Sec.)
15	-15.2	20.2	1.770	4.539
20	-12.5	18.3	1.540	8.119
25	-10.6	16.9	1.370	12.808

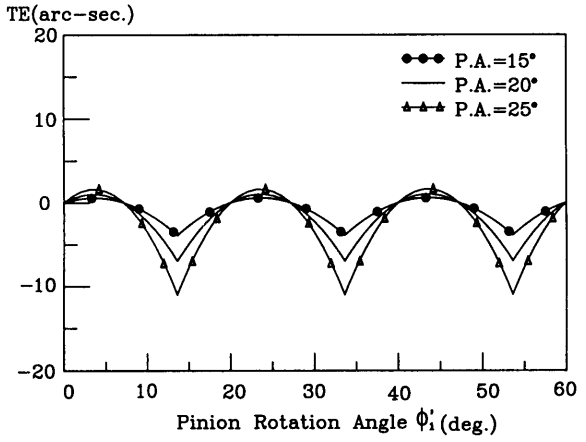

Fig. 6 Transmission errors of the mating gear pair under different pressure angles

mm. Since a larger $R_l^{(G)}$ induces a smaller crowning effect, the CR increases with an increase of $R_l^{(G)}$. In sum, increasing the pressure angle and/or helix angle decreases CRs; increasing the radius of curved-template $R_l^{(G)}$ slightly increases the CR. We also found that the CR decreases as the radius of circular-arc rack cutter R_G increases.

Figure 6 and Table 6 summarize the effects of pressure angle on the CRs and TEs. As mentioned earlier, a smaller pressure angle leads to a higher CR. Table 6 also verifies this phenomenon. As the pressure angle is 15°, the TE is 4.539 arc-sec. The TEs are 8.119 and 12.808 arc-sec., respectively, as the pressure angles are 20° and 25°. In brief, the proposed modified helical gear set with a smaller pressure angle receives a lower level of TE in one meshing cycle.

4.3 Variation of radius center of the circular-arc rack cutter

According to our results, the proposed circular-arc rack cutter that generates the gear results in a built-in parabolic TE even under an ideal meshing condition. Furthermore, TCA simulation results indicate that varying the location of the radius center of the circular-arc rack cutter changes the shape and magnitude of the TE curves. As Fig. 2(a) depicts, the variation of radius center $O_R^{(G)}$ moves along the vertical direction only and its displacement Δx could be either positive or negative, i.e., moving up or down from its original position $O_R^{(G)}$. Thus, the new radius

Table 7 Contact ratios and transmission errors with different amounts of displacement Δx

Δx (mm)	Begin Contact (Deg.)	End Contact (Deg.)	Contact Ratio	Transmission Error (Arc-Sec.)
1.0	-12.5	18.2	1.535	7.970
0.5	-12.5	18.2	1.535	8.044
0.0	-12.5	18.3	1.540	8.119
-0.5	-12.5	18.3	1.540	8.035
-1.0	-12.5	18.3	1.535	8.112

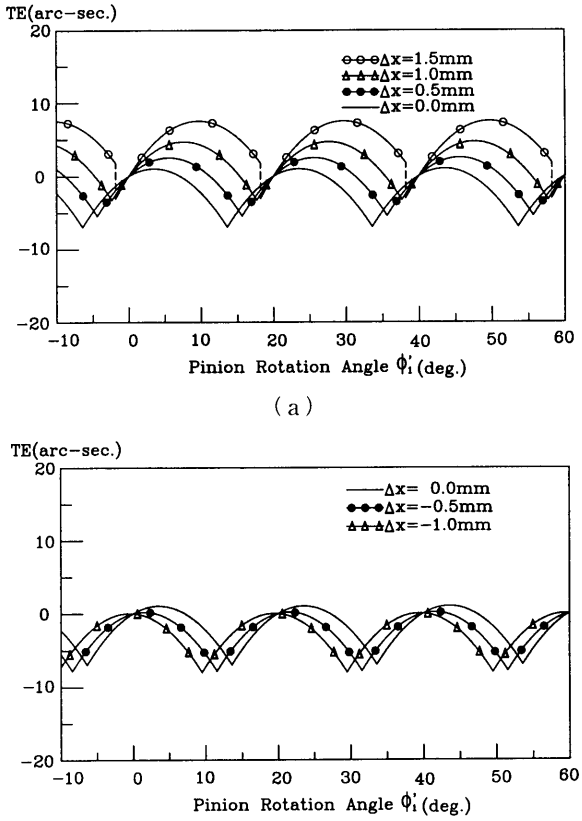

Fig. 7 Transmission errors of the mating gear pair with different rack cutter displacement of Δx

R_G' can be calculated according to the geometrical relationship. For brevity, the detailed derivations for the new mathematical models and related equations are not listed here.

Table 7 displays the CRs and TEs of the helical gear set when the radius center $O_R^{(G)}$ of circular-arc rack cutter is displaced with an amount of Δx. Our simulation results reveal that the TE curves shift to the upper-right when a positive displacement Δx is present, as shown in Fig. 7(a). Thus, the mean value of TE within one meshing cycle increases with a positive displacement of Δx. On the contrary, according to Fig. 7(b), the TE curves shift to the lower-left when a negative displacement of Δx is present. As listed in Table 7, the peak-to-valley values of the TE

curves under the cases, $\Delta x = 0.0$ mm, -0.5 mm and -1.0 mm, are 8.119, 8.035 and 8.112 arc-seconds, respectively. These three values of TEs are very close.

Table 7 also reveals that the CRs are only slightly changed when the absolute displacement value of Δx is not greater than 1.0 mm. However, Fig. 7(a) also indicate that the TE curve becomes discontinuous as Δx equals 1.5 mm. The discontinuity of TE may lead to a higher noise level and should be avoided in practical applications. In sum, the displacement Δx of $O_R^{(G)}$ induces the shift of TE curves and may also change the mean value of TE in one meshing cycle. However, the displacement Δx of $O_R^{(G)}$ should be chosen in a reasonable region to prevent the unfavorable discontinuity of TE curves.

5. Conclusions

This study investigates the CRs, contact teeth, and TEs of the proposed modified helical gear pair, consists of an involute pinion and a modified circular-arc gear. The CR and TE of the gear pair, which are closely related to the gear's noise and dynamics, are calculated according to the TCA simulation. Several illustrative examples demonstrate how the gear design parameters and assembly errors affect the CR and TE of the modified helical gear pair. Based on our simulation results, we conclude the following:

(1) TCA computer program has been developed and applied to calculate the CR and TE of a helical gear set that exhibits point contact due to profile modification;

(2) The contact teeth for the proposed modified helical gear set are less than two during the meshing process, and thus it is not a high-contact-ratio gear set;

(3) A shorter center distance assembly and/or a smaller pressure angle of the gear set results in a higher CR;

(4) A gear set meshing under a positive vertical misaligned angle may possess a higher CR, whereas any horizontal misalignment appears to decrease the CR;

(5) A larger radius of curved-template $R_l^{(G)}$ results in a smaller modification on tooth profiles and, meanwhile, the CR increases slightly; and

(6) Displacement Δx of radius center $O_R^{(G)}$ induces the shift of the TE curves. However, an improperly chosen Δx may cause discontinuity of TE curves.

Acknowledgements

The authors would like to thank the National Science Council of the R.O.C. for financially supporting this research under Contract No. NSC 89-2212-E-009-084.

References

(1) Anderson, N.E. and Loewenthal, S.H., ASME Journal of Mechanisms, Transmissions and Automation in Design, Vol. 108 (1986), pp. 119-126.

(2) Pedrero, J.I., Artes, M. and Garcia-Prada, J.C., Mechanism and Machine Theory, Vol. 31, No. 7 (1996), pp. 937-945.

(3) Tsai, M.H. and Tsai, Y.C., Mechanism and Machine Theory, Vol. 33, No. 5 (1998), pp. 551-564.

(4) Litvin, F.L. and Tsay, C.B., ASME Journal of Mechanisms, Transmission, and Automation in Design, Vol. 107 (1985), pp. 556-564.

(5) Litvin, F.L., Theory of Gearing, (1989), NASA Publication RP-1212, Washington D.C.

(6) Litvin, F.L., Gear Geometry and Applied Theory, (1994), Prentice-Hall, New Jersey.

(7) Litvin, F.L., Chen, N.X., Lu, J. and Handschuh, R.F., ASME Journal of Mechanical Design, Vol. 117 (1995), pp. 254-261.

(8) Tsay, C.B., ASME Journal of Mechanisms, Transmissions and Automation in Design, Vol. 110 (1988), pp. 482-491.

(9) Falah, B., Gosselin, C. and Cloutier, L., Mechanism and Machine Theory, Vol. 33, No. 1/2 (1998), pp. 21-37.

(10) Umeyama, M., Kato, M. and Inoue, K., ASME Journal of Mechanical Design, Vol. 120 (1998), pp. 119-125.

(11) Liou, C.H., Lin, H.H., Oswald, F.B. and Townsend, D.P., ASME Journal of Mechanical Design, Vol. 118 (1996), pp. 439-443.

(12) Lin, H.H., Lee, C.W., Oswald, F.B. and Townsend, D.P., ASME Journal of Mechanical Design, Vol. 115 (1993), pp. 171-178.

(13) Kahraman, A. and Blankenship, G.W., ASME Power Transmission and Gearing Conference, Vol. 88 (1996), pp. 381-388.

(14) Elkholy, A.H., ASME Journal of Mechanisms, Transmissions and Automation in Design, Vol. 107 (1985), pp. 11-16.

(15) Litvin, F.L., Chen, J.S., Lu, J. and Handschuh, R.F., ASME Journal of Mechanical Design, Vol. 118 (1996), pp. 561-567.

(16) Bair, B.W. and Tsay, C.B., ASME Journal of Mechanical Design, Vol. 120 (1998), pp. 422-428.

(17) Chen, Y.C. and Tsay, C.B., Journal of the Chinese Society of Mechanical Engineers, Vol. 22, No. 1 (2001), pp. 41-51.

(18) Chen, Y.C. and Tsay, C.B., Journal of the Chinese Society of Mechanical Engineers, Vol. 21, No. 6 (2000), pp. 537-547.

(19) Shigley, J.E. and Mischke, C.R., Mechanical Engineering Design, 5th ed., (1989), p. 539, McGraw-Hill, N.Y.